ISSN 2176-5480

22nd International Congress of Mechanical Engineering (COBEM 2013)
November 3-7, 2013, Ribeirão Preto, SP, Brazil

EXPERIMENTAL VALIDATION OF ACOUSTIC MODE ATTENUATION IN COMBUSTION CHAMBER USING HELMHOLTZ RESONATOR

Luciana Faria Saint-Martin Pereira
Gabriel Costa Guerra Pereira
Rogério Corá
Pedro Teixeira Lacava
Giuliano Gardolinski Venson
Instituto Tecnológico de Aeronáutica, Praça Marechal Eduardo Gomes, 50, São José dos Campos, SP
lpereira@ita.br, gpereira@ita.br, cora@ita.br , placava@ita.br , giuliano.venson@unitau.com.br

Abstract. *It was verified if the resonators positioned radially in relation to the chamber would be able to attenuate longitudinal oscillations during combustion, by convenience. A methodology to empirically validate a Helmholtz resonator design, applied to attenuate acoustic oscillations inside a combustion chamber, was described. The temperature at the inlet of the resonators was measured using thermocouple to estimate the sound velocity, using a software of chemical equilibrium, and them the volume of cavity were calculated and the resonators were constructed. The acoustic characterization of the combustion chamber was done with and without the resonator during combustion. They were performed tests with radial and longitudinal resonators individually and with both together. The results showed that the radial resonator has an efficiency of dampen the longitudinal oscillations (third longitudinal acoustic mode) of 83.0% (approximately 15.3dB), at the frequency that it was designed to attenuate (667Hz). As might be expected, the longitudinal resonator was effective to attenuate the longitudinal oscillation in practically every spectrum of frequency analyzed, with an efficiency of 89.6% (19.7dB), whilst the resonators together have attenuated 95.7% (27.2dB) at the designed frequency (667Hz). In all best result cases for radial, longitudinal and radial & longitudinal resonator together, compared with the curve without the resonator, the amplitude of the peak decreased and was divided into two minor peaks, thus showing that the absorption of the resonator.*

Keywords: *Helmholtz resonator; variable volume; acoustic mode; combustion instability*

1. INTRODUCTION

The combustion instability is a phenomenon that accompanies the combustion devices with high rate of energy release as rocket engines, jet engines, gas turbines and industrial burners. The coupling between the combustion process and the pressure oscillations due to acoustic behavior of the combustion chamber may lead to a low efficiency of rocket engines. The oscillatory operation is undesirable because it can be severe and impede the operation of components, achieving structural parts, increase considerably the rate of heat transfer to the chamber walls, melt and destroy parts of the system leading to the explosion of the chamber. (Santana Jr, 2008)

A special urgency accompanied the study of vibrational combustion in the last 20 to 30 years, in connection with the creation of combustion chambers for rockets and jet engines. (Natanzon, 1999)

Although the problem has been unceasingly studied for the past four decades, no theoretical general rules have yet been established for designing stable combustor systems. Therefore, concerns on combustion instabilities are still present in every chamber design. The sooner this problem is detected during the development phase, the smaller are the additional expenses with delays in the project.

Acoustic cavities such as Helmholtz resonators were successfully used as damping devices for the suppression of combustion oscillations.(Laudien *at al*, 1995 and Guimarães *at al*, 2012)

The objective of this work is to evaluates experimentally whether resonators positioned radially with respect to the combustion chamber has the ability to attenuate longitudinal oscillations generated during the combustion, because in case of rocket systems, for example, it would be much more convenient to position the resonators in the wall of the combustion chamber, than to position in the injector of propellants, as would be in the case of longitudinal resonators.

2. ACOUST TEST ON COMBUSTION CHAMBER

The experimental bench is schematically shown in Fig. 1(a) showing each instrument with brand and model. A sinusoidal acoustic wave, provided by a Function Generator Agilent model 33220A, is amplified by the Sound Amplifier Times One model SL-525 AB4, feeding the Loudspeaker model WPU 1209, manufactured by Selenium, with the membrane diameter of 30.5 mm. The Pressure Transducers captures the pressure fluctuations inside the chamber and transforms into an electrical signal. This sensor type measures the pressure fluctuations relative to the average pressure with an accuracy of 2Pa. The electrical signal from the Kistler piezoelectric Pressure Transducers model 7261 is amplified by the Charge Amplifier Kistler model 5011B. The signals from the piezoelectric transducers, the function

ISSN 2176-5480

generator and the RMS voltage of the loudspeaker were controlled and measured using a data acquisition system, which consists of A Data Acquisition Device, DAQ NI USB 6259, National Instruments, and a Computer, which uses a LabVIEW 7.0 software acquisition program to present the frequency spectrum and the amplitudes of the pressure within the chamber. Based on the Nyquist criterion, the sampling frequency must be set higher than twice the maximum frequency of interest. In general, the tests were conducted for a frequency range between 500-900 Hz with a resolution of 1Hz and sample rate of 10,000 Hz. The charge amplifiers, which are responsible for converting the signal received from the piezoelectric transducers in an electrical signal, are adjusted with a sensitivity of 2mbar/volt for all tests. This provided an acceptable resolution for all resonant modes of interest. The Transducer Position (TP) corresponds to the central position of each module, being TP1, TP2, TP3, TP4 and TP5, plus one transducer at TP6, positioned at the inlet of the loudspeaker, in order to obtain the acoustic pressure data at the inlet of the chamber. Thermocouples, represented by white circles, were placed along the chamber in order to get the inlet temperature of the longitudinal resonators (that is, on TP1) and the inlet temperature of the radial resonator (on TP4), in the middle of each camera module, as well. The dimensions of the chamber are on Fig. 1(b), for further information, see Corá, 2010.

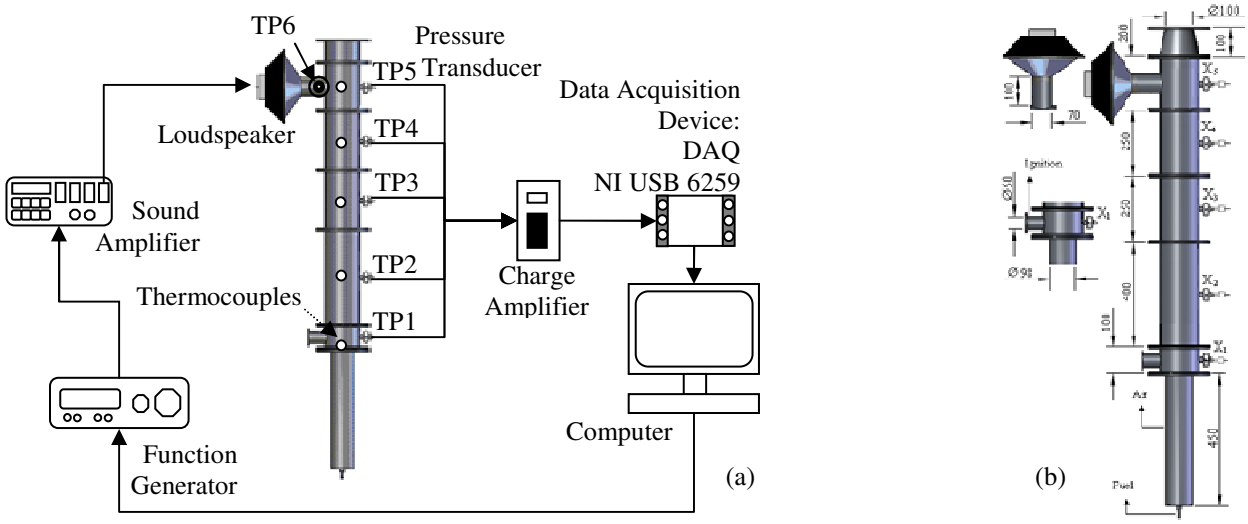

Figure 1. (a) Experimental bench, (b) Combustion chamber dimensions (in mm).

2.1 Resonant frequencies

Acoustic tests with models have shown that the combustion chamber must be treated theoretically as closed/closed system even though the nozzle is not actually closed (Laudien *at al*, 1995). The eigenfrequencies f_{lmn} (in Hz), or natural frequencies, for a cylindrical chamber closed at both sides can be calculated with Eq. (1),

$$f_{lmn} = \frac{c}{2\pi}\sqrt{\left(\frac{\lambda_{mn}}{R_c}\right)^2 + \left(\frac{l\pi}{L_c}\right)^2} \qquad l, m, n = 0, 1, 2, \ldots \tag{1}$$

where lmn are the longitudinal, tangential and radial mode number, respectively, (dimensionless); c is the velocity of sound (in m/s); λ_{mn} is the transverse eigenvalue listed in Tab. 1 for the first few modes, (dimensionless); R_c and L_c are radius and length of the combustion chamber, respectively (in m).

Table 1. Transversal eigenvalue (Laudien *at al*, 1995).

	m					
n	0	1	2	3	4	5
0	0	1.8412	3.0542	4.2012	5.3176	6.4156
1	3.8317	5.3314	6.7061	8.0152	9.2824	10.5199
2	7.0156	8.5363	9.9695	11.3459	12.6819	13.9872
3	10.173	11.706	13.1704	14.5859	15.9641	17.3128

The variation of the speed of sound will alter the natural frequencies of the acoustic modes in the combustion chamber, as showed in Eq. (1). A variation in the combustion equivalence ratio ϕ will alter the temperature of the combustion, and it will change the speed of sound, as showed in Fig. 2 for methane, estimated by Gaseq. Consequently, the change in the speed of sound will alter the natural frequencies of the acoustic modes in the combustion chamber.

ISSN 2176-5480

The combustion equivalence ratio is defined as the ratio between the number of atoms of oxygen present in the stoichiometric reaction and the number of atoms of oxygen present in the real reaction. Thus, a value of $\phi < 1$ (poor combustion) represents a combustion process with less fuel (or more air) than the stoichiometric case. Otherwise, a value of $\phi > 1$ indicate a rich combustion. (Carvalho Jr and Lacava, 2003)

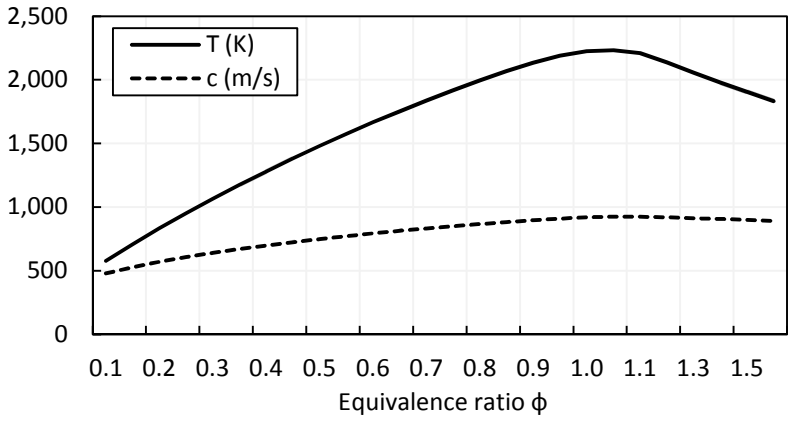

Figure 2. Variation of the speed of sound as a function of ϕ.

2.2 Helmotz resonator

Acoustic cavities such as Helmholtz resonators were successfully used as damping devices for the suppression of combustion oscillations. Resonator consists of a small volume connected with the combustion chamber through an orifice. If the dimensions of the resonator are small in comparison to the wavelength of the oscillation, the gas motion behavior in the resonator is analogous to a mass-spring- damper system (Guimarães *at al*, 2012). The resonant frequency f_0 can be calculated from the geometrical dimensions (Fig. 3) as (Laudien *at al*, 1995)

$$f_0 = \frac{c}{2\pi}\sqrt{\frac{S}{V(l+\Delta l)}} \tag{2}$$

where S is the cross section of the orifice (m^2), l the orifice lengh (m), V the cavity volume m^3, and Δl the mass correction (m), which is (Frendi *et al*, 2005):

$$\Delta l \approx 0.85d \tag{3}$$

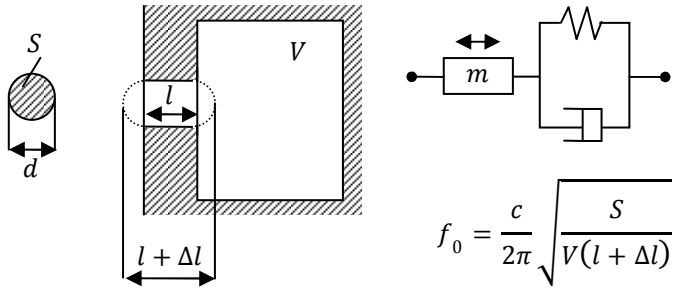

Figure 3. Helmholtz resonator.

To study the acoustical behavior of the resonators, and specially its absorption effect, impedance Z must be determined. This impedance is, in general, a complex unit consisting of the sum of an acoustic resistance R and an acoustic reactance χ:

$$Z = R + i\chi \tag{4}$$

The acoustic impedance is determined by the geometric and mechanical properties of the resonator, in particular the oscillating mass in the orifice, the spring stiffness of the volume and the resistive element associated with viscous

ISSN 2176-5480

dissipation in the orifice. The reactance χ, in $kg/(m^2.s)$, can be written in terms of the cavity dimensions as (Laudien *at al*, 1995)

$$\chi = 2\pi f\rho(l + \Delta l)\left(1 - (f_0^2/f^2)\right) \tag{5}$$

where f is frequency (Hz) and ρ is density of the combustion gas in the chamber (kg/m^3). The Resistance R, in $kg/(m^2.s)$, is a function of the orifice length as well as the dynamic viscosity of the gas derived from the combustion, and is defined as (Laudien *at al*, 1995)

$$R = 4(\varepsilon + l/d)\sqrt{\mu\rho\pi f} \tag{6}$$

where μ is dynamic viscosity of the combustion gas in the chamber, in $Pa.s$, and ε is the resistance factor (dimensionless), which will be discussed later.
When χ and R are multiplied by A/S, one obtains the specific resistance r and reactance x (dimensionless):

$$x = \chi\frac{A}{NS} \tag{7}$$

$$r = R\frac{A}{NS} \tag{8}$$

where A is the cross-sectional area of the combustion chamber (m^2), S the cross cross-sectional area of the orifice (m^2) and N is the number of the tuned absorbers around the circumference of the combustion chamber. Once the impedance is known, the absorption coefficient α and the conductance ξ (real part of the admittance) can be evaluated as (Laudien *at al*, 1994):

$$\alpha = \frac{4r}{\rho c}\Big/\left[\left(1 + \frac{r}{\rho c}\right)^2 + \left(\frac{x}{\rho c}\right)^2\right] \tag{9}$$

$$\xi = \frac{r}{\rho c}\Big/\left[\left(\frac{r}{\rho c}\right)^2 + \left(\frac{x}{\rho c}\right)^2\right] \tag{10}$$

The calculation of the resistance factor ε is not very clear in the literature. Several bibliographies were searched and the resistance factor ε was calculated according to Blackman, 1960, as follows:

$$\log_{10}(\Delta_{nl}/d) = -1.685 + 0.0185(dB) \tag{11}$$

where dB is the pressure measured at the position nearest to the resonator in dB. It was chosen the experimental value equal to $17mbar$ (or $158dB$) for both the longitudinal and radial resonator. From the above equation it is calculated that $(\Delta_{nl}/d) = 17$, then it is calculated ε as:

$$\varepsilon = 1 + (\Delta_{nl}/d) \tag{12}$$

Thus, it was considered $\varepsilon = 20$. This value is also consistent with the value calculated using the procedure described by Ingard, 1953.

2.3 Frequencies of combustion instability

Combustion instabilities have been classified in two major categories: high-frequency instability and low-frequency instability (Santana Jr., 2008). According to Pikalov (2001), the frequencies are classified as low-frequency when the wavelength of the pressure oscillation (λ_0) is much larger than the dimensions of the chamber and as high-frequency when the wavelength is approximately equal or smaller than chamber length.

$$\lambda_0 = c/f_o \tag{13}$$

ISSN 2176-5480

2.4 Positioning of the resonator

The resonator should be positioned in the region of greatest pressure amplitude. Thus, it is important to know the pressure response in a slender duct closed at both sides, similar to the one of this study, which can be given by (Beranek and Vér, 1992)

$$\psi_j = \cos\frac{j\pi z}{L_c} \qquad j = 0,1,2,\ldots \tag{14}$$

where ψ is the amplitude (dimensionless), z is the displacement along the chamber length (in m) and j = acoustic mode (dimensionless).

3. RESULTS

The Nyquist Frequency for this experiment is equal to 2×900 Hz, that is, 1,800 Hz. This corresponds to 1,800 samples per second, or 1.8 kS/s. The DAQ NI USB-6259 has used his 1.25MS/s divided by 8 channels is equal to 156 kS/s for each channel. That is, 156 kS/s is much greater than the Nyquist frequency of 1.8 kS/s, and therefore, the DAQ satisfies the Nyquist criterion for this experiment, thus avoiding the aliasing.

Table 2 compares the natural frequencies calculated using Eq. (1) with those frequencies measured experimentally through the chamber, using the pressure transducer, showing agreement between them, with an error less than 1%.

Table 2. Natural frequencies of acoustic modes in the combustion chamber.

Mode	Theoretical frequency (Hz)	Experimental frequency (Hz)	Error (%)
3L	634	630	0,67
4L	845	845	0,04

The resonators were designed to a frequency of the third longitudinal acoustic mode, with reactive flow, that is, with combustion. The equivalence ratio (ϕ) was chosen experimentally. They were made tests with different values of ϕ using methane (CH4) as fuel, in order to select the ϕ of highest pressure amplitude, with and without acoustic stimulation (Fig. 4), being chosen $\phi = 0.15$.

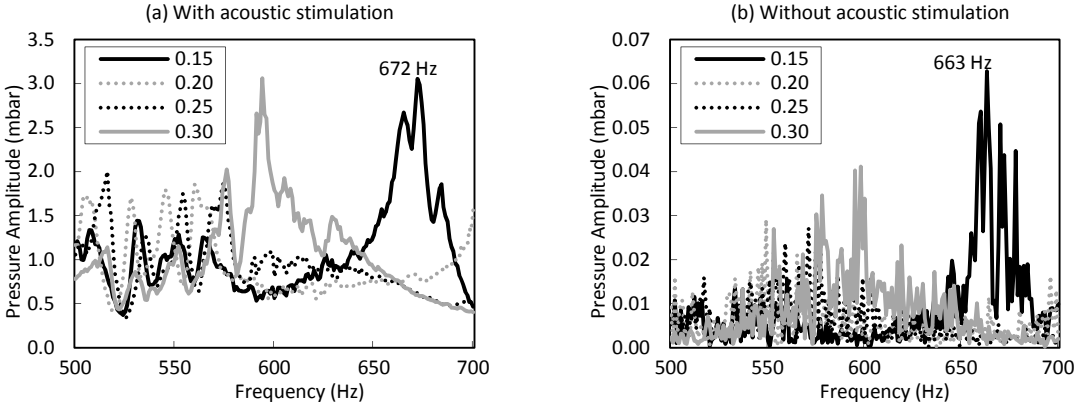

Figure 4. Combustion with different equivalence ratios, (a) With and (b) Without acoustic stimulation.

Figure 3 shows that the behavior of the pressure amplitude is the same with (Fig. 3a) and without (Fig. 3b) acoustic stimulation, but with acoustic stimulation the curve of pressure amplitude is amplified in approximately 100 times. These curves were extracted at TP1 with $\phi = 0.15$. The other positions have similar behavior.

The f_0 was obtained experimentally. Figure 6 shows the pressure amplitudes, with pressure transducer from TP1 to X5, with $\phi = 0.15$, with and without acoustic stimulation. Note that the pressure amplitudes are amplified with acoustic stimulus and that in both cases there are highest frequencies close to 667 Hz. So, it was chosen $f_0 = 667$Hz.

Although the adiabatic temperature of the flame is T = 709.3K for $\phi = 0.15$, it is known that the temperature varies within the chamber. So, it is very important to know the temperature at the inlet of the neck of the resonator, to calculate the sound velocity and, therefore, the volume of the cavity of the resonator.

ISSN 2176-5480

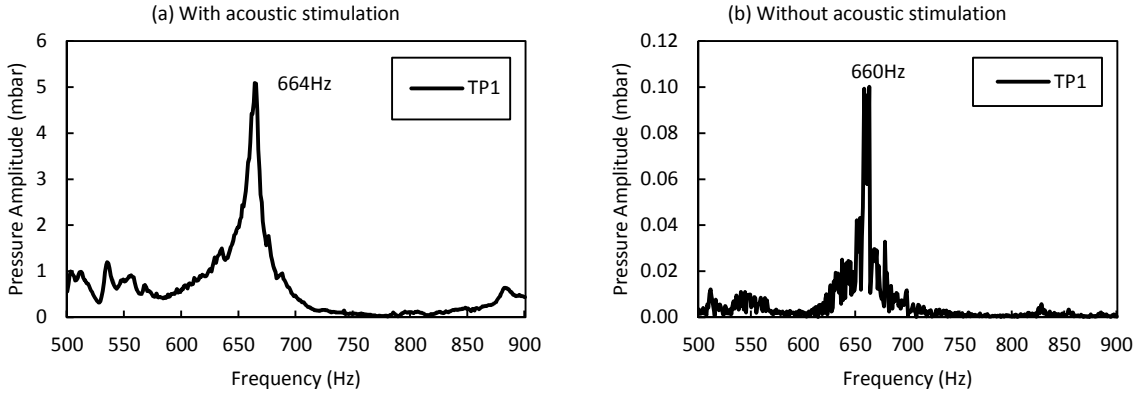

Figure 5. Test with combustion, (a) with and (b) without acoustic stimulus at TP1 position, with $\phi = 0.15$.

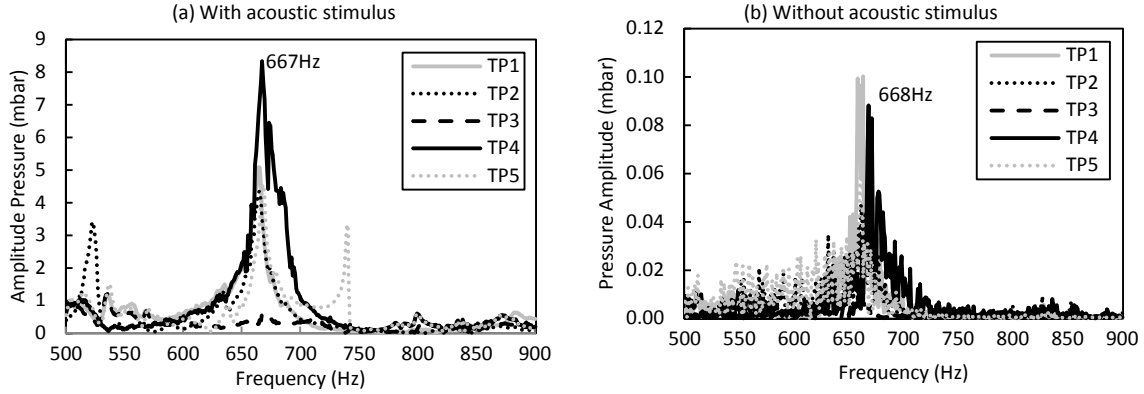

Figure 6. Frequencies of TP1 to TP5, with $\phi = 0.15$ for choice of f_0: (a) with and (b) without acoustic stimulation.

Thus, the average temperature was obtained by thermocouples type k and the results are showed on Tab. 3. It is noted that the average values of temperature are very close to the values obtained in the frequency at which the resonator will be designed. So, it was decided to design the resonators using the temperature on 667Hz. The thermocouple T2 was being used for the ignition system, and because of that, the measured value not appears on table. Thus, the resonators were designed according to Tab. 4.

Table 3. Average temperature throughout the chamber.

Thermocouple	Average Temperature (°C)	Temperature on 667Hz (°C)
T1	147.9	146.7
T2	-	-
T3	171.4	171.9
T4	165.7	165.5
T5	146.2	144.9
T6	136.3	133.7
T7	110.6	109.4

The dimensions of the resonator are small in comparison to the wavelength of the oscillation, once the largest dimension, which is D, represents less than 10% of λ, as showed on Tab. 5. Thus, the gas motion behavior in the resonator is analogous to a mass-spring- damper system.

The dimensions of the combustion chamber, that is, the radius and the length, respectively, are showed on Tab. 6. From Tab. 6, it can be noted that frequencies of the combustion instability can be classified as high-frequency once the wavelength $\lambda_0 = 0.792\text{m}$ is smaller than the chamber length $L_c = 1.250\text{m}$.

ISSN 2176-5480

Table 4. Helmholtz resonator design.

Longitudinal	Radial
$d = 0.012m$	$d = 0.012m$
$l = 0.030m$	$l = 0.030m$
$D = 0.030m$	$D = 0.044m$
$T = 146.7°C$	$T = 133.7°C$
$c = 409.6m/s$	$c = 405.0m/s$
$V = 2.7 \times 10^{-5}m^3$	$V = 2.6 \times 10^{-5}m^3$
$L = 0.038m$	$L = 0.017m$

Table 5. Dimensions of designed Helmholtz resonator.

Dimensions	Percentage of λ
$d = 0.012m$	1.5%
$l = 0.030m$	3.8%
$D = 0.044m$	6.7%
$\lambda = 0.792m$	-

Table 6. Dimensions of combustion chamber.

Data	Measured in combustion chamber
$R_c = 0.075m$	Radius of the chamber
$L_c = 1.250m$	Effective length of the chamber
$X1 = 0.100m$	Length of X1 module
$X2 = 0.400m$	Length of X2 module
$X3 = 0.250m$	Length of X3 module
$X4 = 0.250m$	Length of X4 module
$X5 = 0.200m$	Length of X5 module
$X_{eg} = 0.050m$	Height effective of the cone that exhausts the combustion gases
$R_{eg} = 0.050m$	Radius of the cone that exhausts the combustion gases

The Absorption Coefficient has its optimum at 100%, while the Conductance, by definition, has no limitation. Figure 7 shows the spectral behavior of the absorption coefficient as well as the conductance for three different absorber arrangements in a closed tube. If the system had the damping optimized taking into account only the absorption coefficient, would be suggestive to choose the arrangement with higher absorption, that is, with 12 resonators. On the contrary, if taken into account the maximization of the conductance, the best configuration would be 24 or more resonators. Acoustically speaking, more than 12 resonators overdamp this system, which implies in less than 100% absorption, but increase the width of the frequency band absorbed. The most usual approach is to optimize the damping by the absorption coefficient, despite the uncertainties of this model due to the non homogeneity of the field of acoustic pressure (Laudien at al, 1994). Thus, it was decided to the arrangement of 12 resonators. Figure 7 is for the longitudinal resonator, but for the radial resonator, the behavior is very similar.

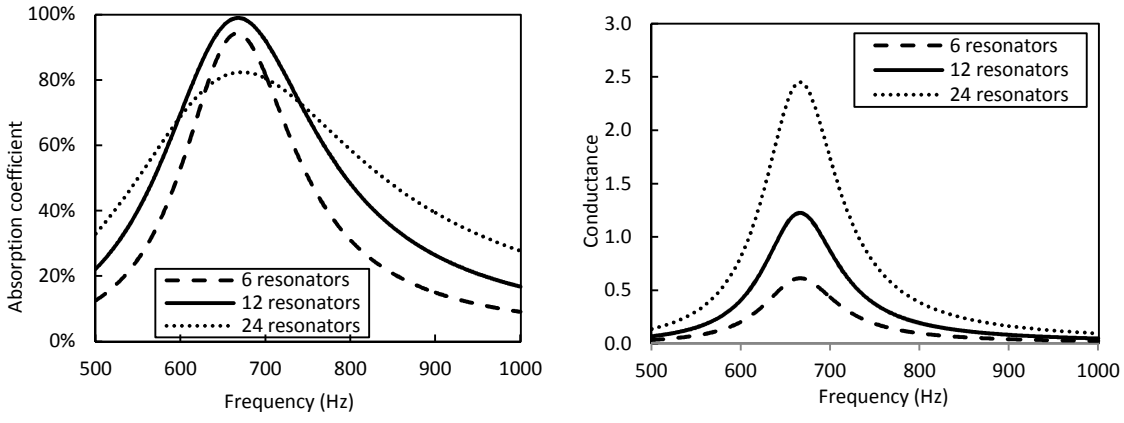

Figure 7. Absorption behavior of an under (6), optimized (12) and overdamped (24) system.

ISSN 2176-5480

Figure 8 shows the locations of nodes and anti-nodes, extracted from Eq. (14). The 5 positions of the pressure transducers are represented by a black circle. The locations of the resonators row are represented by a triangle.

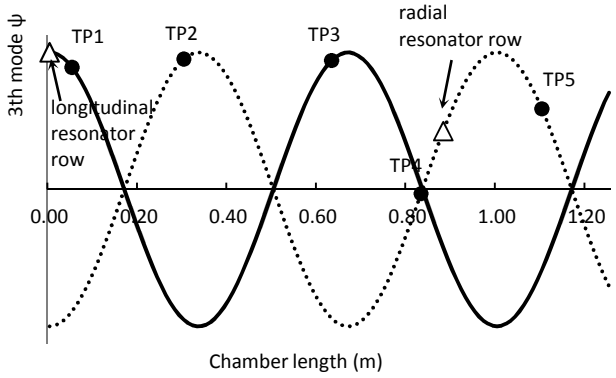

Figure 8. Choosing the position of the resonator.

In the position $z = 0.000$m the amplitude is maximum and so, at this point the longitudinal resonator was coupled. The ideal would be to couple the radial resonators in a position where the amplitude is maximal, that is, in an anti-node, but they were positioned in $z = 0.875$ m (Fig. 8), close to a node. Nevertheless, the chamber is not completely closed-closed because the upper side has an aperture of 30% of the diameter of the chamber in order to exhaust the combustion gases. Thus, the curve might change and therefore the position of the node shall shift slightly.

The volume of the longitudinal resonators (Fig. 9a) is different from the volume of the radial resonators (Fig. 9b). Both resonators have variable volume.

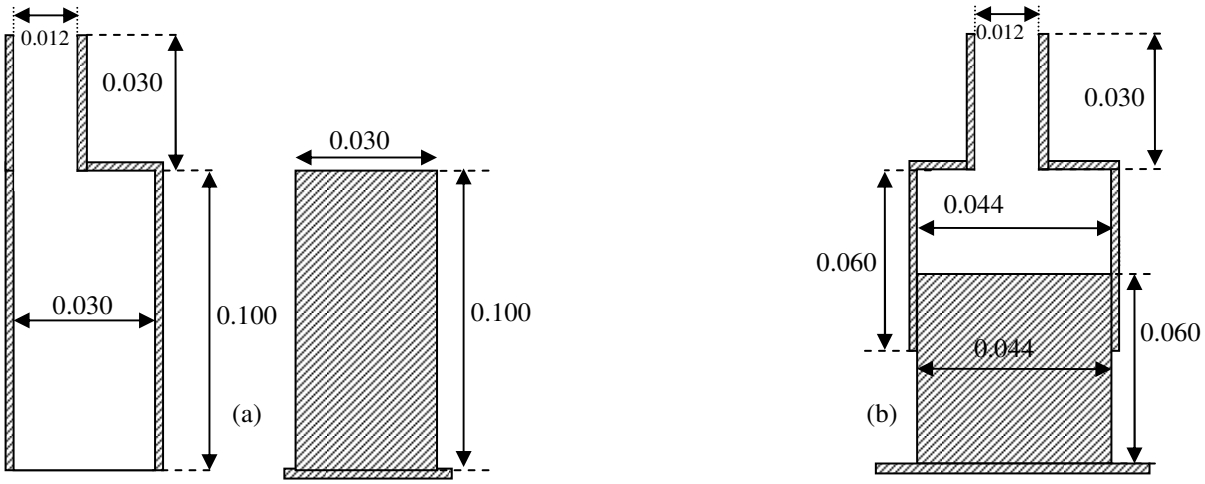

Figure 9. (a) Longitudinal and (b) radial resonator with variable volume.

The resonators were coupled in two configurations, being them, radial resonator (Fig. 10a), positioned in the wall of the combustion chamber and, longitudinal resonator positioned in the injector (Fig. 10b). Tests were performed with radial and longitudinal resonators individually, and then, with both resonators together. Figure 10c shows the combustion chamber inside an acoustic enclosure, to muffle the loud noise of the tests.

Figure 11 shows the pressure amplitudes for the transducer at the 5 different positions, on the same scale, whilst the Fig. 12 and Fig. 13 shows the pressure amplitudes for the transducer at the 2 best positions.

By Fig. 11 it is observed that TP1 showed the best results for radial resonators, absorbing not only at the frequency on which the resonator was designed to absorb (667Hz), but also for a large range of frequency around 667Hz. The higher amplitude was divided into two smaller ones, thus showing the resonator absorption. TP4 and TP5 showed some amplifications.

ISSN 2176-5480

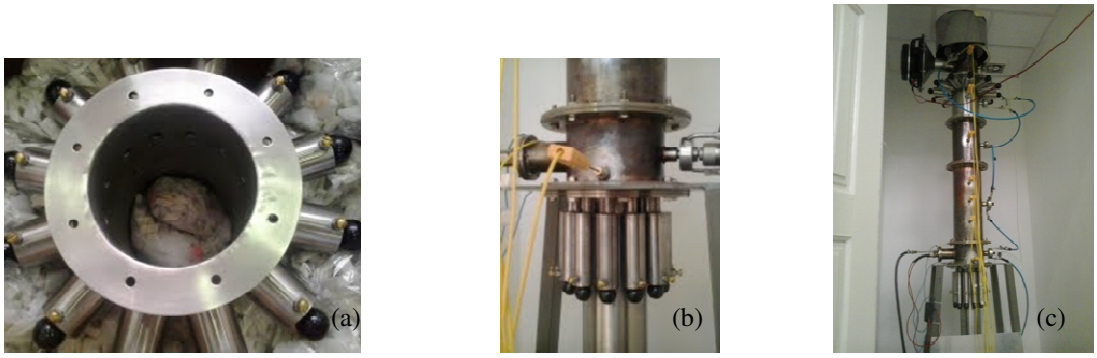

Figure 10. (a) Longitudinal resonator, (b) Radial resonator and (c) Combustion chamber.

Figure 11 show also that all positions presented great amplitudes without resonator, except for the position TP3. It can be concluded, therefore, that there is probably an anti-node near all positions, except for TP3, which is probably close to a node.

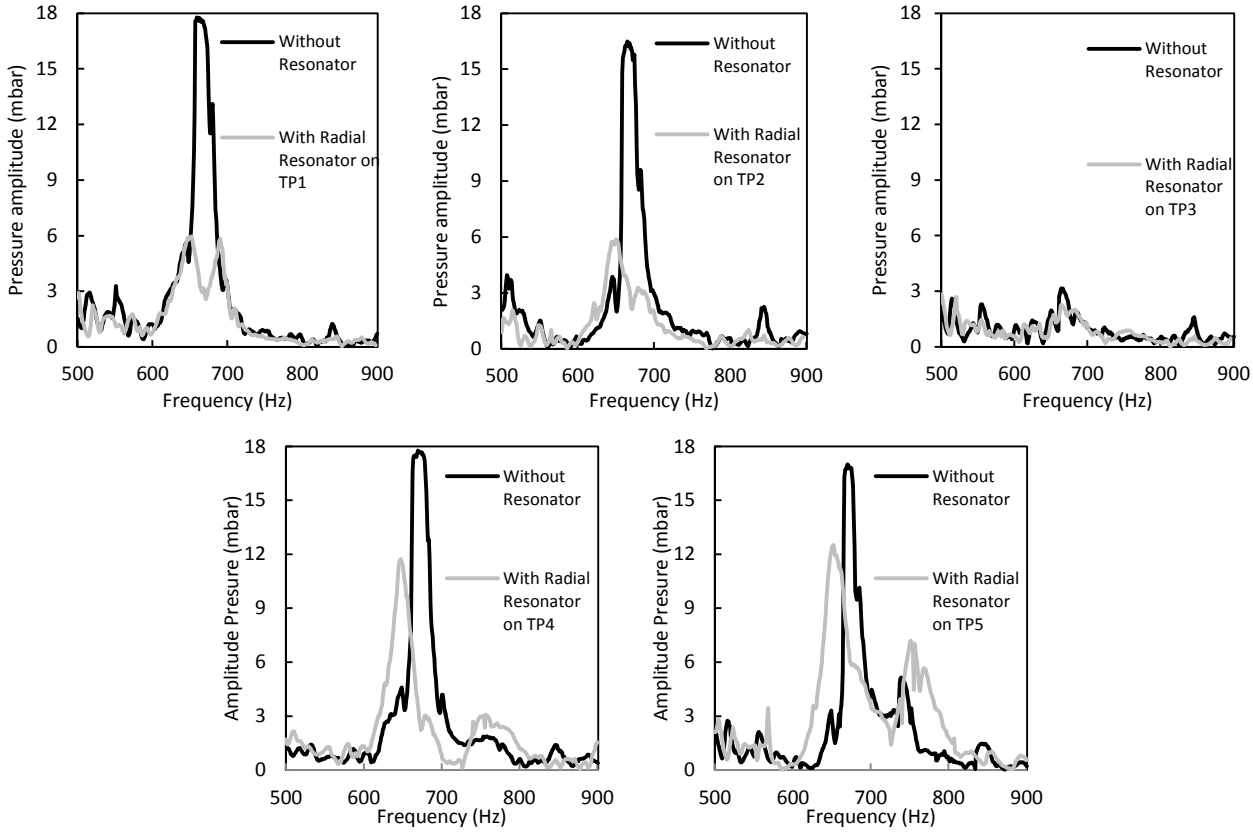

Figure 11. Results with radial resonators at 5 different Transducer Positions (TP).

Figure 12 shows that TP2 and TP5 showed the best results for longitudinal resonators, absorbing at the frequency designed to absorb (667Hz), and also at a width range of frequency near 667. The higher amplitude was divided into two smaller ones, as well. A similar result can be seen in the Fig. 13 for the resonators together.

The highest amplitudes of each position are listed on Tab. 7. It may be noted, for both configurations of the radial and longitudinal resonators, that the smallest amplitudes appeared at TP3, whereas the greatest amplitudes appeared at TP4. So, as was discussed, TP3 might be near a node whilst TP4 might be near an anti-node. However, when comparing these results with those from Fig. 8, it is otherwise noted that TP3 is near an anti-node whilst TP4 is near a node. Maybe this is happening because there is a node for the 4th mode close to TP3, and therefore, it can be influencing. Thus, it is concluded that the approximation that uses the equation of closed-closed tube, Eq. (14), may not be adequate to determine where the nodes and anti-nodes are. Probably, a numerical analysis of finite elements may give a more accurate result of these positions.

ISSN 2176-5480

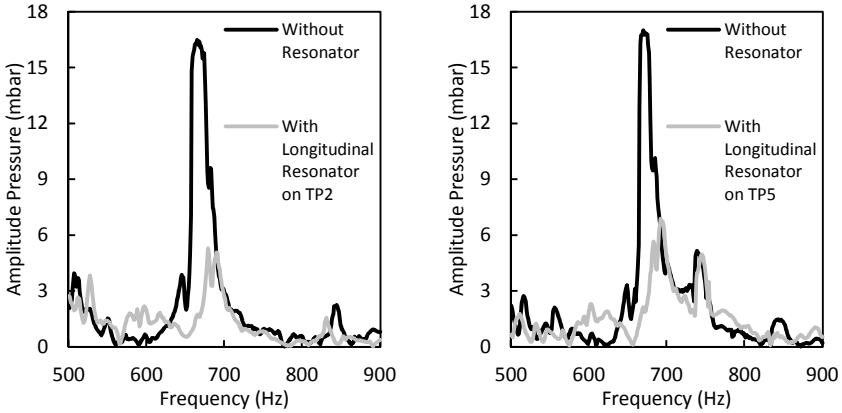

Figure 12. Results with longitudinal resonators for the 2 best transducer positions.

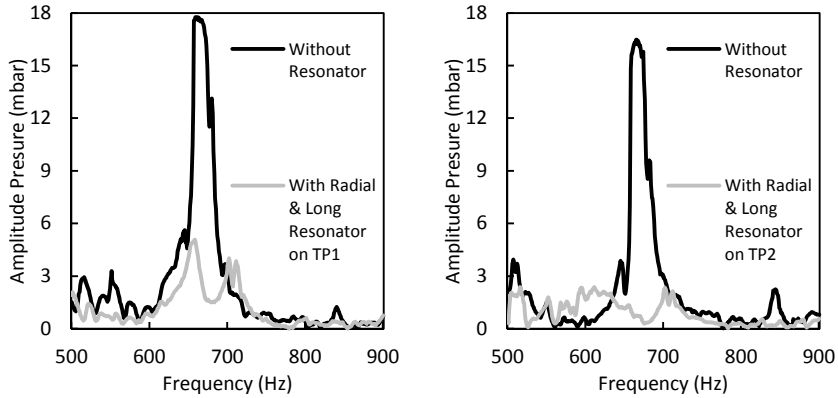

Figure 13. Results with radial and longitudinal resonators for the 2 best transducer positions.

Table 7. Highest pressure amplitudes in each position.

	TP1	TP2	TP3	TP4	TP5
Radial highest amplitudes (mbar)	6.0	5.9	2.8	11.7	12.5
Longitudinal highest amplitudes (mbar)	15.4	5.3	3.4	10.9	6.9
Radial and longitudinal highest amplitudes (mbar)	5.1	2.4	2.4	7.7	9.7
Transistor position (m)	0.050	0.300	0.625	0.875	1.100

Table 8 shows how the resonators have absorbed, in each position, for the frequency in which they were designed to absorb (667Hz). It can be observed that with the use of the resonators radial and longitudinal, separated or together, there were reductions in the amplitude compared to the situation without resonator, in all positions.

Table 8. Amplitudes in 667 Hz for each position.

	X1	X2	X3	X4	X5
Without resonator (mbar)	17.6	16.4	3.0	17.4	16.0
With radial resonator (mbar)	3.0	3.9	2.2	4.2	8.9
With longitudinal resonator (mbar)	4.7	1.7	2.9	6.6	1.7
With radial and longitudinal resonator (mbar)	2.7	0.7	0.5	3.2	7.1

Figure 14 summarizes the best absorptions for (a) radial, (b) longitudinal and (c) radial & longitudinal resonator, compared with the curve without the resonator, being them: 83.0% of absorption for radial resonator, 89.6% for longitudinal resonator and, 95.7% for both together, at 667Hz. To obtain those absorptions in dB, it was taken an approximation using the equation $20.\log(P_{out}/P_{in})$, were pressure at chamber inlet is 8.0mbar, according to TP6. In this way, the best results were: 15.3dB of absorption for radial, 19.7dB for longitudinal and, 27.2dB for both.

ISSN 2176-5480

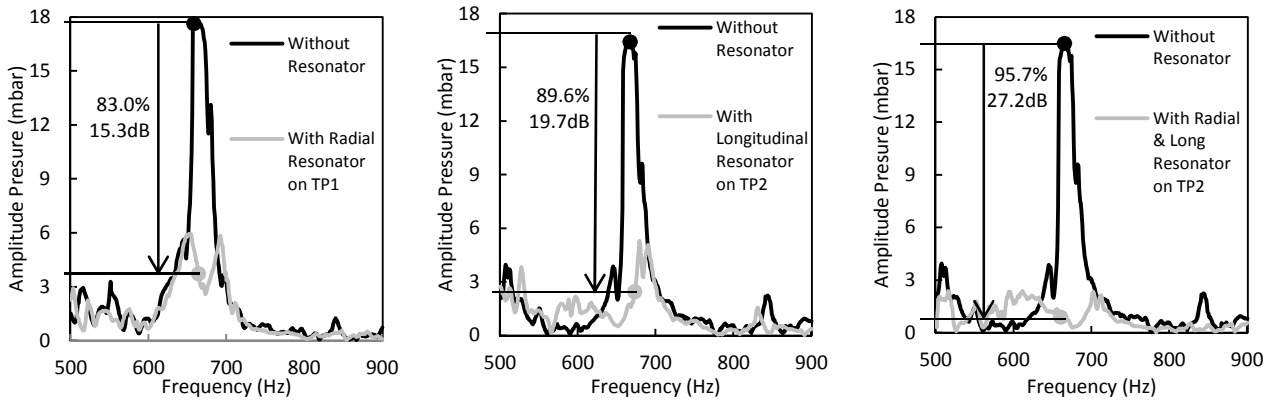

Figure 14. Best results for (a) radial, (b) longitudinal and (c) radial and longitudinal resonators on 667Hz.

4. CONCLUSIONS

The present work evaluated experimentally whether resonators positioned radially with respect to the combustion chamber has the ability to attenuate longitudinal oscillations generated during the combustion, because in case of rocket systems, for example, it would be much more convenient to position the resonators in the wall of the combustion chamber, than to position in the injector of propellants, as would be in the case of longitudinal resonators.

It was established a mathematical formulation to design resonators for control of acoustic instabilities with possible application in liquid propellant rocket engines. Based on this methodology, two systems were designed, built and tested, being them longitudinal and radial resonators.

The results show that the radial resonator alone has an efficiency of dampen the longitudinal oscillations of 83.0% (approximately 15.3dB), which is smaller than the longitudinal resonator, of 89.6% (or 19.7dB), in the frequency that it was designed to absorb (667Hz). As might be expected, the longitudinal resonator was effective to mitigate the oscillations in practically every spectrum of frequency analyzed. The combination of the resonators was positive, attenuating in 95.7% (27.2dB) the frequency of project (667dB).

5. REFERENCES

Agilent 33220A, Function Waveform Generator. “Data Sheet”. 11 Sep. 2013 <http://agilent.33220A>.

Beranek, L. and Vér, I., 1992. *Noise and Vibration Control Engineering*. John Wiley & Sons, Toronto.

Blackman, A. W., 1960. “Effect of Nonlinear Losses on the Design of Absorbers for Combustion Instabilities”. *ARS Journal*, Vol. 30, n. 11, p. 1022-1028. Sep. 2013 < www.aiaa.org>.

Carvalho Jr, J. A. and Lacava, P. T., 2003. *Emissões em Processos de Combustão*. Unesp Publishing House.

Corá, R., 2010. *Controle Passivo de Instabilidades de Combustão Utilizando Ressonadores de Helmholtz*. Ph.D. thesis, Instituto Tecnológico de Aeronáutica, São José dos Campos.

Frendi, A., Nesman, T. and Canabal, F., 2005. “Control of Combustion-Instabilities Through Various Passive Devices”. In *Proceedings of the 11th AIAA/CEAS Aeroacoustics Conference - ARC2005*. Monterey, New York.

GASEQ, 2005. “Chemical Equilibrium Program in Perfect Gases”, v. 0.79. Sep. 2013 <http://www.gaseq.co.uk/>.

Guimarães, G. P., Pirk, R., Souto, C. D., Rett, S. R. and Góes, C. S., 2012. “Acoustic Modes Attenuation on Rocket Engines Using Helmholtz Ressonators: Experimental Validation”. In *Proceedings of the 15th International Conference on Experimental Mechanics - ICEM2012*. Porto, Portugal.

Kistler, “Single-Channel Multi-Range Laboratory Charge Amplifier”. Sep. 2013. <www.kistler.com>

Kistler, “Piezoelectric Low Pressure Sensor - Very High Sensivity - Pressure Range 10 bar”. Sep. 2013 <www.kistler.com>

Langel G., Laudien E., Pongratz R. and Habiballah M., 1991. “Combustion Stability Characteristics of the Ariane 5 L7 Engine”. In *Proceedings of the 42nd Congress of the International Astronautical Federation - IAC1991*. Montreal, Canada.

Laudien E., Pongratz R., Pierro R. and Preclik D., 1994. “Experimental Procedures Aiding the Design of Acoustic Cavities”. *Liquid Rocket Engine Combustion Instability*. Progress in Astronautics and Aeronautics, Vol. 169, p. 377-399.

Natanzon, M. S. and Culick F. E. C., 1999. *Combustion Instability*. Moscow, Russia.

National Instruments, DAQ NI USB 6259. “High-Speed M Series Multifunction DAQ for USB - 16-Bit, up to 1.25 MS/s, up to 80 Analog Inputs”. Sep. 2013 <http://ni.com>.

Santana Jr., A., 2008. *Investigation of Passive Control Devices to Suppress Acoustic Instability in Combustion Chambers*. Ph.D. thesis, Instituto Tecnológico de Aeronáutica, São José dos Campos.

Sound Amplifier, Times One: SL 525 AB4, 2005. “Amplificadores - Series SL, Classe AS”. 17 Sep. 2013 <www.advancesom.com.br>.

Pikalov, V. P. and Dranovski, M. L., 2001. *General Principles to Evaluation of High-frequency Combustion Instability in Liquid Rocket Engines*. Russia.

6. RESPONSIBILITY NOTICE

The author(s) is (are) the only responsible for the printed material included in this paper.